

Effect of Rolling Temperature on Microstructure and Mechanical Properties of a Nb-Mo Microalloyed Medium Mn Steel

Shan Liu^a, Wenxia Li^a, Junhua Su^a, Yunpeng Wang^a, Minghui Cai^{a,b,*}

^aSchool of Materials Science and Engineering, Northeastern University, Shenyang 110819, China

^bKey Laboratory of Lightweight Structural Materials, Liaoning Province, Northeastern University, Shenyang 110819, China

Received: November 25, 2018; Revised: May 14, 2019; Accepted: May 19, 2019

Warm rolling of medium Mn steel is a promising technology to meet the needs of vehicle weight reduction and energy conservation while ensuring the safety for passengers. In this study, a novel Nb-Mo microalloyed 6.6Mn steel was subjected to a series of warm rolling tests at temperatures ranging from 630 to 690 °C, based on the thermodynamic-based prediction of inter-critical annealing using a Thermo-Calc software. As a comparison, a conventional multi-stage thermo-mechanical process involving hot rolling, cold rolling and inter-critical annealing was carried out as well. The optimal rolling temperature parameters for warm rolling was explored through tensile tests and the detailed microstructural characterization. The experimental results show that the microstructure and mechanical characteristics strongly depended on the warm rolling temperature. A better combination of UTS and TE products (~32.0 GPa·%) was achieved in the 660°C-warm-rolled specimen, which is much higher than 12.3 GPa·% for the hot formed 22MnB5 steel and is also comparable to 38.3 GPa·% for the annealed cold-rolled specimens.

Keywords: *Medium Mn steel, warm rolling, microstructure, mechanical properties.*

1. Introduction

In the past few years, the automotive industry has been searching for high/ultrahigh strength steels with good ductility to reduce the weight of vehicles while increasing its crashworthiness^{1,2}. For example, the most commonly used boron steel (22MnB5) for hot forming exhibited an ultimate tensile strength (UTS) of ~1,500MPa and quite low total elongation (TE) of ~6% in the martensitic state³. Recent research mainly focused on improving the ductility of hot formed steels by either introducing a post-hot forming tempering treatment for 22MnB5 or developing an alternative class of hot formed steels such as a medium Mn steel⁴. In the latter case, UTS and TE in the ranges of 1330-1448 MPa and 16.7~25.3% can be achieved after applying hot forming (HF) cycles at 700 °C due to an additional TRIP effect and grain ultra-refinement of constituent phases (ferrite, austenite and martensite).

These new processing routes may offer a new opportunity for practical production of ultrahigh strength medium Mn steel, in view of the heavy springback during cold rolling⁵⁻⁸. As demonstrated in our preliminary work, dozens of passes in the cold rolling of medium Mn steel were required to reduce the sheet thickness from 4 to 1 mm. Therefore, to reduce the number of process operations, it may be of interest to use an alternative route, i.e. only several-pass warm rolling. However, the potential of warm rolling of medium Mn steel has not yet been researched in detail so far.

In this study therefore, a novel Nb-Mo microalloyed medium Mn steel was subjected to a series of warm rolling tests at temperatures ranging from 600 to 720°C, and compared with the commercial hot formed Mn steels and the conventional multi-stage thermo-mechanical process including hot rolling, cold rolling and intercritical annealing. The detailed microstructural evolution was investigated by scanning electron microscopy (SEM), electron backscatter diffraction (EBSD) and X-ray diffraction (XRD), etc., and uniaxial tensile tests were performed for optimizing the warm rolling temperature parameters.

2. Experimental Procedure

The experimental steel with composition of Fe-0.17C-6.6Mn-1.1Al-0.05Nb-0.22Mo (wt.%) was prepared in a laboratory vacuum induction furnace. The equilibrium phase fraction as a function of temperature was determined from the TCFE5 database in Thermo-CalcTM, as referred in our preliminary work⁶. Based on this work, the A_3 temperature was determined as 752 °C, and the amount of austenite in equilibrium and retained at room temperature was also summarized in Table 1, together with the corresponding concentrations of C and Mn in austenite. The maximum amount of austenite retained at room temperature was approximately 38% after quenching from 660 °C.

*e-mail: cmhing@126.com

Table 1. The calculated phase fraction of austenite in equilibrium and retained at room temperature, together with the concentrations of C and Mn in austenite for each individual rolling temperature.

T , °C	V_γ in equilibrium		C in γ	Mn in γ	V_γ at room temp. %
	%		%		%
630	45		0.42	12.5	20
660	55		0.35	10.8	38
690	70		0.29	9.8	23

T -temperature; V_γ -the volume fraction of austenite.

The 50 Kg ingot was forged after austenitization at 1200 °C for 1 h, and cut into small plates with sectional area of 100 mm×100 mm. Afterwards, rough hot rolling was carried out to produce the plates of ~8.5 mm in thickness, followed by immediate quenching in oil. After machining the decarburized layers on both sides, small billets with a cross-section of 35 mm×65 mm and a thickness of ~7 mm were heated to 850 °C for 20 min, followed by air cooling to the desirable warm rolling temperature range from 630 to 690 °C. The total rolling reduction was ~80% with four passes. After each pass, reheating was required to ensure that the plate was soaked at the same temperature for 5 min before the next rolling pass.

Microstructural observations were performed using SEM, EBSD and XRD. Specimens for SEM and EBSD were prepared following the standard mechanical polishing. In the final step, samples were finished with a colloidal silica attack-polishing agent (OPS). SEM and EBSD were performed using a field-emission gun (FEG) SEM (Zeiss-Supra 55VP, Germany) integrated with an angle-selective backscattered (AsB) and EBSD detectors. A step size of 50 nm was selected for indexing and EBSD maps were acquired on the longitudinal section including the rolling and normal directions of samples. Post processing of EBSD data using the HKL Channel 5 software. The fraction of retained austenite was determined using XRD method with Cu-K α radiation following the ASTM method.

Tensile specimens with a gauge length of 5 mm and cross section of 6 × (~2) mm were machined from the WRed strips with tensile axis (TA) parallel to the rolling direction (RD). Uniaxial tensile tests were carried out on an INSTRON 5967 30kN machine at a constant strain rate of 5×10⁻⁴ s⁻¹. The engineering stress-strain curves were analyzed to determine the values of yield strength (YS), ultimate tensile strength (UTS) and total elongation to fracture (EI).

3. Results and Analyses

3.1 Microstructural evolution

The representative AsB maps of the WRed specimens at different temperatures are shown in Fig.1. It was found that rolling temperature had a strong effect on the final microstructures, which can be compared by their substructure development as well as martensitic transformation to austenite.

As the specimen was warm rolled at 630 °C, the lamella with indistinct grain boundaries were observed, as shown in Fig. 1. The mean spacing of lamella was approximately 100 nm, which was thought to be associated with incomplete fragmentation of the deformed martensite by dislocation rearrangement during warm rolling^{9, 10}. As the rolling temperature rose to 660 °C, the deformed ferrite with sharp grain boundaries (Fig. 1b) was observed, which was mainly attributed to the continuous absorption of dislocations into the low-angle boundaries. The degree of substructure development reflected the extent of recovery of the deformed martensite. With further raising the rolling temperature to 690 °C, the martensite packets in some localized regions were observed, which originated from the partial martensitic transformation from austenite upon cooling due to a loss of thermal stability of retained austenite (Fig. 1c).

For a detailed analysis on the influence of warm rolling temperature on the final microstructural parameters, EBSD mapping was performed as well. The representative phase distribution and grain boundary misorientation maps as a function of rolling temperature are shown in Fig. 2. The phase maps clearly show the change in the fraction of retained austenite (V_γ) with rolling temperature, indicating that the V_γ value first increased and then decreased with increasing rolling temperatures from 630 to 690 °C, which mainly depended on the fraction of austenite in equilibrium and the change in alloying concentrations (e.g. C and Mn elements) in austenite with temperature. This experimental result is in accordance with the above-predicted one, i.e. the maximum austenite fraction was obtained after warm rolling at ~660 °C. Considering the accuracy of EBSD measurement, the amount of retained austenite was further determined and analyzed based on the following XRD data.

According to quantitative EBSD analysis, a relatively higher fraction of BCC phase (ferrite or martensite) with low angle grain boundaries (LAGBs) (~52.9%) was found in the 630°C-WRed specimen (as marked by the black line in Fig. 3a), which is consistent with the above-mentioned incomplete recrystallization behavior. In comparison, the fraction of bcc phase with LAGBs dropped significantly to ~38.5% in the 660°C-WRed specimen (as marked by the red line in Fig. 3a), which was thought to be associated with further recrystallization of the deformed bcc phase.

With further increasing rolling temperature to 690 °C, the fraction of bcc phase with LAGBs reached ~36.8% (as marked by the blue line in Fig. 3a), which was closely related to the formation of a large fraction of thermal martensite upon cooling. In contrast, as the warm rolling increased from 630 to 660 °C, the fraction of BCC phase with LAGBs dropped by ~10%, implying the occurrence of dynamic globalization during reverse transformation from the deformed martensite to austenite.

In order to compare the volume fraction of retained austenite at different rolling temperatures, a quantitative XRD analysis was performed. Fig. 4 shows the XRD patterns of these WRed specimens at three different rolling temperatures. The volume fraction of retained austenite was calculated from the integrated intensities of (111) γ , (200) γ , (220) γ , (311) γ peaks of austenite, and those of (110) α , (200) α , (211) α , (220) α peaks of ferrite.

The volume fraction of retained austenite was estimated by the following equation:

$$V_{\gamma} = (I_{\gamma}/R_{\gamma}) / [(I_{\gamma}/R_{\gamma}) + (I_{\alpha}/I_{\alpha})] \quad (1)$$

where V_{γ} is the volume fraction of retained austenite, I_{γ} is a theoretical parameter that is proportional to the theoretical integral strength; R_{γ} are integrated intensity per angular diffraction peak (hkl) in the α -phase or the γ -phase, respectively.

Similar to EBSD data, the amount of retained austenite first increased and then decreased with increasing rolling temperature from 630 to 690 °C. The 630-WRed specimen contained ~16.0% retained austenite, which is lower than the value (~21%) in the 660-WRed specimen. After warm rolling at 690 °C. The amount of retained austenite slightly dropped to ~18%.

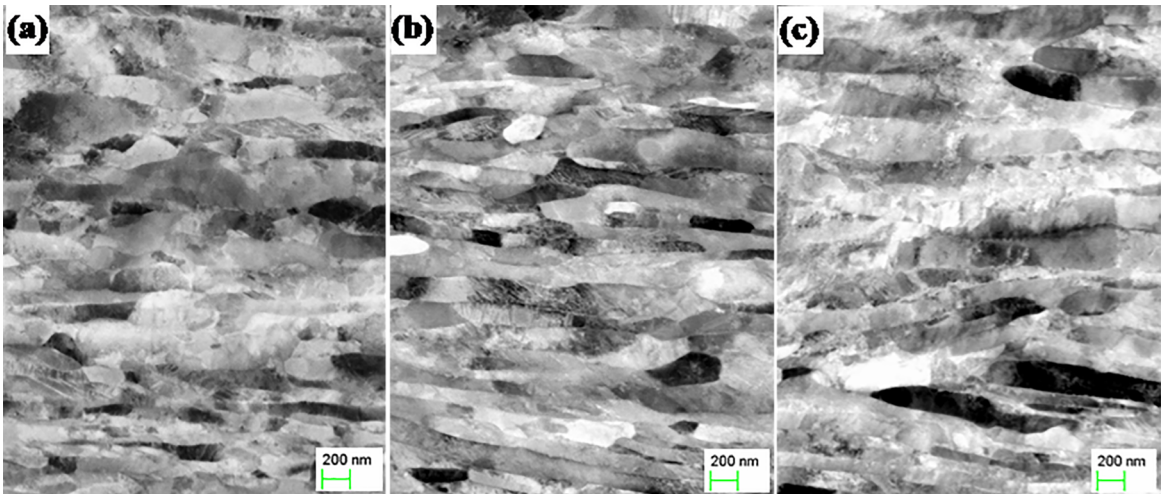


Figure 1. AsB maps of a 0.17C-6.6Mn-1.1Al-0.05Nb-0.22Mo steel processed by warm rolling at various temperatures: (a) 630 °C, (b) 660 °C and (c) 690 °C.

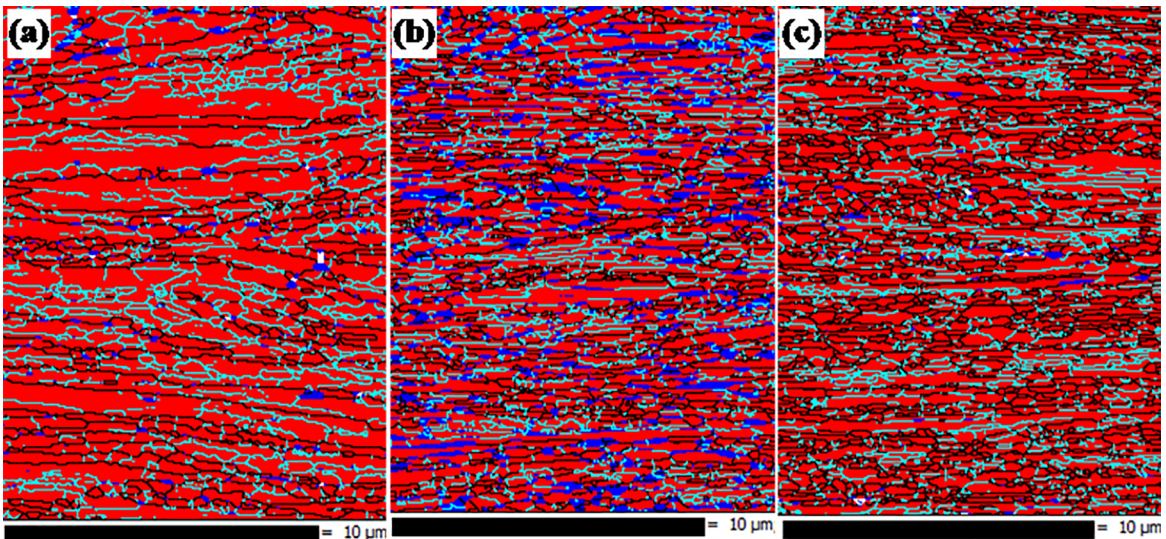


Figure 2. Phase distribution and grain boundaries of a 0.17C-6.6Mn-1.1Al-0.05Nb-0.22Mo steel processed by warm rolling at various temperatures: (a) 630 °C; (b) 660 °C and (c) 690 °C. BCC-red; FCC-blue; HAGBs (>15°)-solid black line; LAGBs (2~15°)-solid green line.

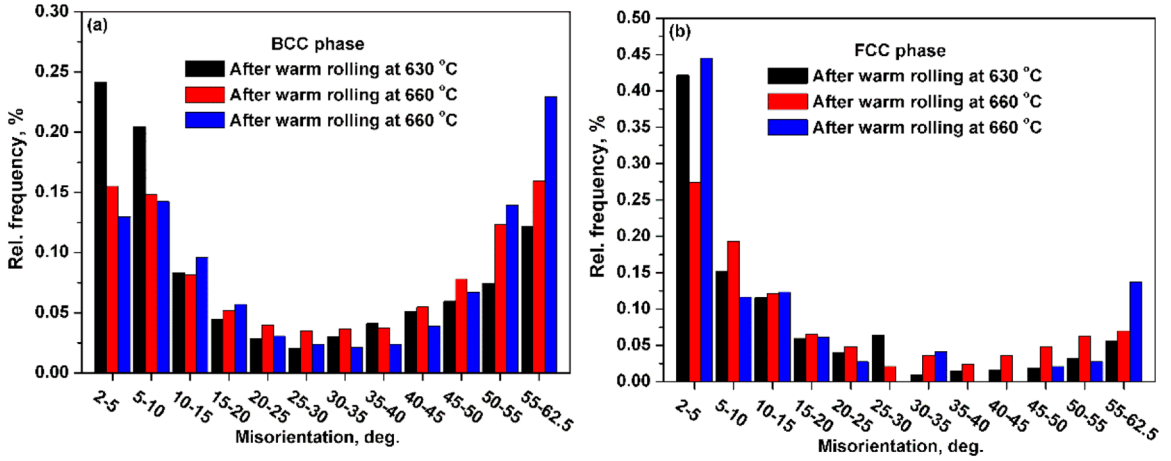


Figure 3. Grain boundaries misorientation distribution profiles for both BCC(a) and FCC(b) phases in a 0.17C-6.6Mn-1.1Al-0.05Nb-0.22Mo steel processed by warm rolling at 630, 660 and 690 °C.

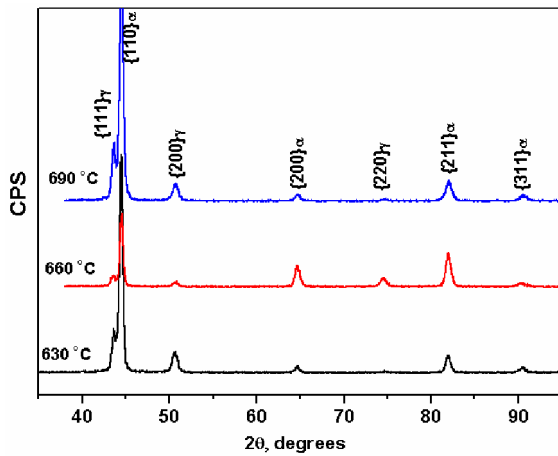


Figure 4. X-ray diffraction patterns of a 0.17C-6.6Mn-1.1Al-0.05Nb-0.22Mo steel processed by warm rolling at temperatures ranging from 630 to 690 °C.

3.2 Tensile properties

The tensile engineering stress-strain curves of all WRed specimens are shown in Fig.5, illustrating a significant dependence of tensile properties on warm rolling temperature. As warm rolling was performed at 630 °C, the specimen exhibited both high yield strength (YS>1100 MPa) and ultimate tensile strength (UTS>1100MPa), but the yield ratio was quite high (YS/UTS>0.9), due to the absence of work hardening caused by the ultrafine BCC structure mixed with the retained austenite with relatively high mechanical stability. After warm rolling at 690 °C, the mechanical stability of retained austenite was so low that it quickly transformed to martensite at low strain levels, corresponding to continuous yield behavior and extremely high initial work hardening rate.

As a result, the specimen exhibited extremely high UTS of ~1,600 MPa and limited tensile ductility (TE) of ~16%. Surprisingly, the 660 °C-WRed tensile specimen exhibited an obvious yield point extension due to the localized deformation, followed by a sustained work hardening behavior occurring over the large strain range from ~5.5% to ~22.5%. Thus, an excellent combination of both high UTS (~1420 MPa) and good ductility (~22.5%) was achieved in this case. In comparison, a better combination of UTS (>1,420~1,600 MPa) and high ductility (>16~22.5%) was achieved after warm rolling above 660 °C without any further annealing. The product of UTS and TE ranged from 25.6 to 32.0 GPa·%, which is much higher than 12.3 GPa·% for the HF 22MnB5 steel ⁴, and is also comparable to 38.3 GPa·% for the annealed CR specimen ⁷.

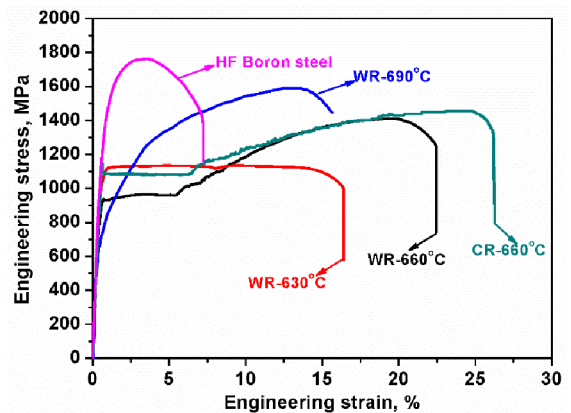


Figure 5. Engineering stress-strain curves of a 0.17C-6.6Mn-1.1Al-0.05Nb-0.22Mo steel processed by warm rolling at temperatures ranging from 630 to 690 °C, together with those of HFed 22MnB5 steel [4] and the CRed specimen after annealing at 660 °C for 30 min [7].

4. Discussion

Many researches have shown that the overall mechanical properties of medium Mn steel are proportional to the volume fraction of retained austenite partly due to the TRIP effect⁹. The present work however, shows that the V_γ ranged from ~16% to ~21%, implying no significant difference in the fraction of retained austenite, regardless of warm rolling temperature. Therefore, our medium Mn steel exhibited a remarkable change in mechanical response among these warm-rolled specimens at three various temperatures, which reflected the rolling-temperature-dependence of the TRIP effect or the mechanical stability of the retained austenite.

It is known that there exists a direct relationship between work hardening rate and the rate of martensitic transformation in metastable austenitic stainless steels^{6,10,11}. The higher is the transformation rate, the higher is the work hardening rate. Similarly, the ductility of medium Mn steel can be also improved by the TRIP effect, because the high work hardening caused by TRIP can delay the necking behavior, and can also aid in strain accommodation¹². Thus, it may be reasonable to evaluate the martensitic transformation behavior corresponding to the mechanical stability of the retained austenite by analyzing the flow behavior. As described in Section 3.1, the 630°C-WRed structure experienced incomplete fragmentation due to quite slow diffusion rate of C and Mn, resulting in the ultrafine ferrite + martensite + retained austenite duplex structure with a high fraction of LAGBs. Meanwhile, the retained austenite exhibited so high mechanical stability that it hardly transformed to martensite upon tensile straining. In this case, this deformation behavior of the 630°C-WRed specimen was characterized by almost no work hardening, which is similar to what was observed in the UFG ferrite structure produced by severe plastic deformation (SPD) or dynamic transformation. In contrast, as the rolling temperature was raised to 690 °C, the as-rolled microstructure was composed of ferrite and retained austenite, together with a large fraction of thermal martensite. Also, the mechanical stability of austenite was reduced due to the decreased concentrations of C and Mn in austenite and the growth of austenite grains. Thus, the TRIP effect was complete at quite low strain levels, resulting in high UTS but limited ductility. However, partial dynamic globalization of the deformed martensite occurred during warm rolling at 660 °C, i.e. a heterogeneous lamellar and granular ($\alpha+\gamma$) duplex structure was formed in this case. The microstructural-level inhomogeneity serves as the initial imperfection, triggering strain partitioning and finally shear band localization upon tensile straining¹³. Thus, it can be inferred that the excellent properties of the 660 °C-WRed specimen was mainly attributed to the combined effects of a heterogeneous duplex structure, together with the sustained TRIP effect occurring during plastic deformation.

In summary, the present study demonstrates that warm rolling without any subsequent inter-critical annealing can not only improve the mechanical properties of medium Mn steels, but also the surface quality of the final steel plates. The combined effects of rolling temperature on the overall properties of medium Mn steel resulted from the following aspects, i.e. phase constituent, the fraction of retained austenite and the mechanical stability of retained austenite^{6-8,14,15}. In particular, the multiple Nb-Mo microalloying plus warm rolling may be a promising method for the development of a new generation of advanced high-strength medium Mn steel.

5. Conclusions

This work investigated the influence of warm rolling temperature on the microstructure and mechanical properties of Nb-Mo microalloyed medium Mn steel. The following conclusions could be drawn:

- (1) The WRed medium Mn steel exhibited the lamellar multiphase microstructure, and the microstructural evolution strongly depended on rolling temperature. With increasing warm rolling temperature from 630 to 660 °C. The fraction of bcc phase with LAGBs significantly dropped, due to dynamic globalization of the deformed microstructure. After warm rolling at 690 °C, the decreased fraction of LAGBs was mainly associated with the formation of martensitic transformation upon cooling.
- (2) A better combination of UTS and TE (~32.0 GPa·%) was achieved in the 660 °C- warm-rolled specimen, which is much higher than 12.3 GPa·% for the hot formed 22MnB5 steel, and is also comparable to that of the conventional annealed cold-rolled medium Mn steel.
- (3) The combined effects of warm rolling temperature on the overall properties of medium Mn steels were mainly attributed to the phase constituent, the fraction of retained austenite and its mechanical stability.

6. Acknowledgements

The authors gratefully acknowledge the financial support of Northeastern University College Students' Practice and Training Program (Grant No.180099), Fundamental Research Funding of the Central Universities, China (Grant No.N160204001) and Henan Provincial Science and Technology Cooperation Project, China (No.182106000016) and Natural Science Foundation of China (Grant No. 51401050 & No.U1760205).

7. References

1. Suh DW, Kim SJ. Medium Mn transformation-induced plasticity steels: Recent progress and challenges. *Scripta Materialia*. 2017;126:63-67.
2. Hu B, Luo H, Yang F, Dong H. Recent progress in medium-Mn steels made with new designing strategies, a review. *Journal of Materials Science and Technology*. 2017;33(12):1457-1464.
3. Karbasian H, Tekkayam AE. A review on hot stamping. *Journal of Materials Science and Technology*. 2010;210(15):2103-2118.
4. Rana R, Garson CH, Speer JG. *Proceedings of 5th International Conference on Hot Sheet Metal Forming of High-performance Steel*. Canada: Inhaltsverzeichnis; 2015.
5. Ding R, Dai ZB, Huang MX, Yang ZG, Zhang C, Chen H. Effect of pre-existed austenite on austenite reversion and mechanical behavior of an Fe-0.2C-8Mn-2Al medium Mn steel. *Acta Materialia*. 2018;147:59-69.
6. Cai MH, Li Z, Chao Q, Hodgson PD. A novel Mo and Nb microalloyed medium Mn TRIP steel with maximal ultimate strength and moderate ductility. *Metallurgical and Materials Transactions: A*. 2014;45:5624-5634.
7. Cai MH, Zhu WJ, Stanford N, Pan LB, Chao Q, Hodgson PD. Dependence of deformation behavior on grain size and strain rate in an ultrahigh strength-ductile Mn-based TRIP alloy. *Materials Science and Engineering: A*. 2016;653:35-42.
8. Pan HJ, Cai MH, Ding H, Huang HS, Zhu B, Wang YL, et al. *Materials Design*. 2017;134:352-360.
9. Suh DW, Kim SJ. Medium Mn transformation-induced plasticity steels: Recent progress and challenges. *Scripta Materialia*. 2017;126:63-67.
10. Herrera C, Ponge D, Raabe D. Design of a novel Mn-based 1 GPa duplex stainless TRIP steel with 60% ductility by a reduction of austenite stability. *Acta Materialia*. 2011;59:4653-4664.
11. Beladi H, Cizek P, Hodgson PD. Dynamic recrystallization of austenite in Ni-30 Pct Fe model alloy: Microstructure and texture evolution. *Metallurgical and Materials Transactions: A*. 2009;40:1175-1189.
12. Lee YK, Han J. Current opinion in medium manganese steel. *Materials Science and Technology*. 2015;31(7):843-856.
13. Choi KS, Soulami A, Liu WN, Sun XW. Influence of various material design parameters on deformation behaviors of TRIP steels. *Computational Materials Science*. 2010;50(2):720-730.
14. Suh DW, Park SJ, Lee TH, Oh CS, Kim SJ. Influence of Al on the microstructural evolution and mechanical behavior of low-carbon, manganese transformation-induced-plasticity steel. *Metallurgical and Materials Transactions: A*. 2010;41(2):397-408.
15. Luo HW, Shi J, Wang C, Cao WQ, Sun XJ, Dong H. *Acta Materialia*. 2011;59:4002-4014.